EPJ Web of Conferences **206**, 06004 (2019) https://doi.org/10.1051/epjconf/201920606004
ISMD 2018

Recent Results from the CERN LHC Experiment TOTEM

Implications for Odderon Exchange

T. Csörgő, for the TOTEM Collaboration[1,2,3,*]

[1]MTA Wigner FK, H-1525 Budapest 114, P.O.Box 49, Hungary
[2]EKE KRC, H-3200 Gyöngyös, Mátrai út 35, Hungary
[3]CERN, CH-1211 Geneva 23, Switzerland

Abstract. Recent results are summarized from the TOTEM experiment at CERN LHC, including measurements of the total, elastic and inelastic cross-sections, the nuclear slope parameter B, the differential cross-section of elastic scattering and the real to imaginary part ration ρ at $\sqrt{s} = 2.76$ and 13 TeV. The implications of these data for Odderon (odd-gluon colorless) exchange are discussed.

1 Introduction

Currently, seven experiments are completing their data taking and data analysis programmes at the Large Hadron Collider (LHC), the most energetic particle accelerator made by humans so far. The four general purpose experiments, ALICE, ATLAS, CMS and LHCb are supplemented by three specialized experiments, LHCf, MoEDAL and TOTEM, that focus on forward physics and search for exotic particle states. Five out of these seven experiments, namely ALICE, ATLAS, CMS, LHCb and TOTEM are overseen by the Resource Review Boards of LHC. This report summarizes recent results from the TOTEM experiment (TOTal cross-section and Elastic scattering Measurement), presented at the XLVIII International Symposium on Multiparticle Dynamics, Singapore, in September 2018. In this work, we quote the final TOTEM results, thus this manuscript can also be considered as a brief summary of the results of the four most recent TOTEM publications of refs. [1–4].

2 TOTEM physics and experimental setup

In general, the goal of the TOTEM experiment is to measure colorless exchange, including elastic, single and double diffractive scattering as well as central exclusive production at the energies of the Large Hadron Collider at CERN. These processes correspond to an increasing elastic fraction of the total cross-section and their precise measurement requires special experimental setup in the forward direction, in the LHC tunnel extending as far as 220 m from Interaction Point 5 (IP5), the collision point that is used for measurements by both the CMS and the TOTEM experiments. By the time of writing this manuscript, a common CMS-TOTEM precision proton spectrometer or CT-PPS project, that started as a common CMS - TOTEM effort, has been fully integrated to the CMS experiment and became the PPS project

*e-mail: tcsorgo@cern.ch

of CMS. Although this report summarizes the recent standalone TOTEM results, it is important to mention that the (CT-)PPS project allowed to operate the world's most complex Roman Pot detector system under regular LHC running conditions and resulted in a successful CMS-TOTEM data taking period during LHC Run-2 (2016-2018) with data recorded with tagged forward protons exceeding 100 fb^{-1}. The harvesting of the rich physics potential of the (CT-)PPS dataset has just been started [5].

The TOTEM experimental setup consists of two inelastic telescopes T1 and T2 to detect charged particles coming from inelastic pp collisions and the Roman Pot detectors (RP) to detect elastically scattered protons at very small angles [6]. A RP unit consists of 3 RPs, two approaching the outgoing beam vertically and one horizontally. Each RP is equipped with a stack of 10 silicon strip detectors designed with the specific objective of reducing the insensitive area at the edge facing the beam to only a few tens of micrometers. The 5.4 m (7 m) long lever arm between the near and the far RP units at $\sqrt{s} = 2.76$ TeV (13 TeV) has the important advantage that the local track angles in the x and y-projections perpendicular to the beam direction can be reconstructed with a precision of 2 μrad (3 μrad), respectively.

The inelastic telescopes are placed symmetrically on both sides of Interaction Point 5 (IP5): the T1 telescope is based on cathode strip chambers (CSCs) placed at ±9 m and covers the pseudorapidity range $3.1 \leq |\eta| \leq 4.7$; the T2 telescope is based on gas electron multiplier (GEM) chambers placed at ±13.5 m and covers the pseudorapidity range $5.3 \leq |\eta| \leq 6.5$. The pseudorapidity coverage of the two telescopes at $\sqrt{s} = 2.76$ TeV allows the detection of about 92 % of the inelastic events. As the fraction of events with all final state particles beyond the instrumented region has to be estimated using phenomenological models, the excellent acceptance in TOTEM minimizes the dependence on such models and thus provides small uncertainty on the inelastic rate measurement.

The complete and detailed description of the TOTEM experiment is given in refs [6, 7]. Specific details of the experimental setups used for the recent TOTEM measurements at $\sqrt{s} =$ 2.76 and 13 TeV of the total, elastic and inelastic cross-sections, the nuclear slope parameters are given in refs. [1–4]. Below, we detail only some of the specific modifications of the general TOTEM experimental setup, that were necessary to for the data taking and to achieve the physics goals of the measurements at $\sqrt{s} = 2.76$ and 13 TeV, respectively.

3 Data taking

The Roman Pot (RP) units used for the measurement at $\sqrt{s} = 2.76$ TeV are located on both sides of the IP at distances of ±214.6 m (near) and ±220.0 m (far) from IP5 [4]. The analysis is performed on a data sample (DS1-2.76) recorded in 2013 during an LHC fill with $\beta^* = 11$ m injection optics. The RP detectors were inserted to 13 times the transverse beam size. Although the differential cross-section measurement is based on the analysis of this DS1-2.76 dataset, the total cross-section measurement at $\sqrt{s} = 2.76$ TeV is based on a different data set (DS2-2.76) that was recorded with at similar beam conditions but RP detectors placed at 4.3 times the transverse beam size. This data set DS2-2.76 had higher statistics and it was also used in order to obtain the final normalization of the data set DS1-2.76, as detailed in [4]. The horizontal RP detectors were not inserted during the data taking at $\sqrt{s} = 2.76$ TeV, and the vertical alignment uses the RP position sensors and is further refined with precise constraints based on symmetries of elastic scattering [51].

The RP units used for the measurements at $\sqrt{s} = 13$ TeV are located on both sides of the LHC Interaction Point 5 (IP5) at distances of ±213 m (near) and ±220 m (far) [1]. At $\sqrt{s} = 13$ TeV, the horizontal RP detectors were inserted and their overlaps with the two vertical RPs allowed for a precise relative alignment of the detectors within the unit.

At $\sqrt{s}$ = 13 TeV, the data analysis has been performed on a large data sample, including seven data sets (DS1 - DS7) recorded in 2015 during a special LHC fill with β^* = 90 m optics and detailed in ref. [1]. The RP detectors were placed at a distance of 10 times the transverse beam size (σ_{beam}) from the outgoing beams. The special trigger settings allowed to collect about 10^9 elastic events. The angular resolution was different for each of the data sets DS1-DS7, and it deteriorated with time within the fills, expected mainly due to the beam emittance growth. The data sets have been reorganized according to their resolution into two larger data sets. The ones with better (about 20 %) resolution were collected into DS_g, which includes DS1, DS2 and DS4. The remaining ones are collected in data set DS_o. The normalization of the differential cross-section measurement at $\sqrt{s}$ = 13 TeV is based on the total cross-section measurement at the same energy. The total cross-section analysis was performed on a data set DS_n, that was also measured with a β^* = 90 m optics, but with the RP detectors placed two times closer to the beam, to 5 times the transverse beam size.

We also report on the measurement of the ratio of the real to imaginary part of the forward scattering amplitude, the parameter ρ obtained from a special measurement in the Coulomb-Nuclear Interference (CNI) region [2]. This measurement was based on data taken in September 2016 during a sequence of dedicated LHC proton fills with the special beam properties corresponding to β^* = 2500 m. The vertical RPs approached the beam centre to only about 3 times the vertical beam width, σ_y, corresponding roughly to 0.4 mm. Such an exceptionally close distance was required in order to reach very low $|t|$ values and was possible due to the low beam intensity in this special beam operation: each beam contained only four or five colliding bunches and one non-colliding bunch, with about 5 $\times 10^{10}$ protons in each bunch [2]. The horizontal RP-s were used for the track-based alignment only, and therefore they were placed at a safe distance of 8 times the horizontal beam with, corresponding to about 5 mm. This horizontal distance was close enough to have the horizontal RP overlapping with the vertical RPs [2]. Let us also stress that TOTEM measurements provided a set of consistent values for the total cross-section of proton-proton scattering using three different methods (the inelastic-independent method of refs. [10] and [12], the ρ-independent method of ref. [13] and the luminosity-independent method of ref. [11] at 7 TeV, yielding values of σ_{tot} = 98.3 ± 2.0 mb, 98.6 ± 2.3 mb, as well as 99.1 ± 4.3 mb and 98.1 ± 2.4 mb, respectively. Similar measurements at 8 TeV indicated that our results for the total proton-proton cross-section are stable not only for the choice of the method, also for very different beam conditions as well [9]. The results for various TOTEM cross-section measurements, including the recent results at $\sqrt{s}$ = 2.76 and 13 TeV are summarized in Table 1 and Figure 4, and are discussed in greater details in subsection 5.2, based on a recent and more detailed TOTEM review [1].

4 Elastic analysis

The horizontal and vertical scattering angles of the proton at IP5 (θ^*_x,θ^*_y) are reconstructed in a given arm by inverting the proton transport equations using TOTEM's special LHC optics reconstruction and recalibration method, detailed in ref. [14]. The scattering angles obtained for the two arms are averaged and the four-momentum transfer squared is calculated as $t = -p^2\theta^{*2}$, where p is the LHC beam momentum and the scattering angle $\theta^* = \sqrt{\theta^{*2}_x + \theta^{*2}_y}$. Precise understanding of the proton transport at IP5 is of key importance for the success of the TOTEM experiment. In all the TOTEM analysis presented here, a novel method of optics evaluation is utilized, based on ref. [14], which exploits the kinematic constraints of elastically scattered protons observed in the RPs. Typically we find that the residual uncertainty of

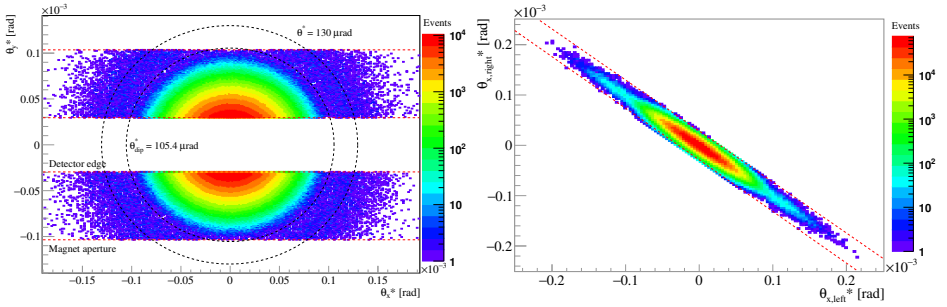

Figure 1. Left panel: Rotational symmetry of elastic scattering in the (θ_x^*, θ_y^*) plane at $\sqrt{s}$ = 13 TeV proton-proton collisions, as measured by TOTEM and detailed in ref. [3]. The red dashed lines show the analysis acceptance cuts, which define the acceptance boundaries near the detector edge and magnet aperture. The inner black dashed circle illustrates the approximate scattering angle position θ^*_{dip} = 105.4 μrad of the diffractive minimum, while the outer black dashed line indicates the approximate scattering angle position of θ^*_{bump} = 130 μrad of the diffractive maximum. **Right panel:** Collinearity of the horizontal scattering angles at the collision point $\theta^*_{\text{x,left}}$ and $\theta^*_{\text{x,right}}$ in elastic pp scattering at $\sqrt{s}$ = 13 TeV proton-proton collisions, as reconstructed by TOTEM [3]. The dotted lines indicates 4σ physics cuts applied to select the elastic events. See ref. [3] for the collinearity cuts on the vertical scattering angle θ^*_y as well as further details on the other analysis cuts.

the optics estimation method is smaller than 0.25%, which makes it possible to determine the total cross-sections with about 2-3 % relative precision.

Instead of detailing this method, let me here just highlight some of its beautiful applications and results. The azimuthally uniform distribution of the scattering angle θ^* demonstrates the azimuthal symmetry of elastic scattering. This is illustrated on Figure 1, which shows the analysis acceptance cuts with red dashed lines, near to the edge of the detector and the aperture of the LHC magnets. On Figure 1 two black circles highlight the quantum interference apparent in these data, that reveal a local scattering minimum and maximum behaviour. These rings, visible by eye even on the raw TOTEM data, clearly indicate a quantum interference pattern in elastic proton-proton scattering at LHC energies. These rings suggests that protons have a composite structure that can be directly observed by quantum interference in elastic proton-proton scattering at LHC energies, see ref. [3] for further details on the corresponding differential elastic cross-section data.

The right panel of Figure 1 indicates the collinearity of the horizontal scattering angle θ^*_x in the left and right going directions in elastic pp scattering at $\sqrt{s}$ = 13 TeV proton-proton collisions, as reconstructed by TOTEM [3]. The dotted lines indicates 4σ physics cuts applied to select the elastic events. Ref. [3] details the collinearity cuts on the vertical scattering angle θ^*_y as well as the other analysis cuts that were defined to select progressively the elastic events.

The selection of elastic events and the main steps of the analysis were similar at 13 and 2.76 TeV: both data analysis started with the reconstruction of kinematics, detector alignment, recalibration of the LHC optical functions with the constraints coming from the measured pp elastic scattering data. The measured differential cross-sections were corrected for resolution unfolding and acceptance, background substraction and detection efficiency, angular resolution, normalization and binning effects [3, 4]. The horizontal and relative near-far alignment was done based on the observed tracks. The analysis at 2.76 TeV was further complicated by the lack of the horizontal RP-s, that made track-based bottom-top RP alignment impossible,

so new methods were developed for absolute y-alignment of the two diagonals. These were based on two constraints from the symmetry of elastic scattering. The first constraint was that the barycenter of the distribution of the θ_y^* scattering angle was aligned to zero. The second constraint was that after rescaling the distribution of the θ_x^* and θ_y^* horizontal and vertical scattering angles should be the same [4]. Fortunately the calibration of the LHC optics was independent from the detector alignment procedure.

5 Results at $\sqrt{s} = 13$ and 2.76 TeV

5.1 Measurement of $(\rho, \sigma_{\rm tot})$ at 13 TeV – implications for Odderon exchange

The TOTEM experiment at the LHC has measured the differential elastic proton-proton scattering cross section down to $|t| = 8 \times 10^{-4}$ GeV^2 at the centre-of-mass energy of $\sqrt{s} = 13$ TeV, using a special LHC optics with $\beta^* = 2.5$ km, as detailed in ref. [2]. This allowed TOTEM to access the Coulomb-nuclear interference (CNI) region and to determine ρ, the real-to-imaginary ratio of the hadronic scattering amplitude at $t = 0$ with an unprecedented precision.

Measurements of the total proton-proton cross-section and ρ have been published in the literature from the low energy range of $\sqrt{s} \approx 10$ GeV up to the LHC energy of 8 TeV [15]. Such experimental measurements have been parametrised by a large variety of phenomenological models in the last decades, and were analysed and classified by the COMPETE collaboration [16].

One of the most inspiring recent observation of TOTEM indicates the presence of a crossing-odd component in the scattering amplitude of pp and $p\overline{p}$ elastic collisions at the LHC energies, the so called Odderon effect, proposed in 1973 by Lukaszuk and Nicolescu [17]. Figure 2 of TOTEM [2] indicates one of the indirect Odderon effects. This Figure clearly demonstrates, that none of the models considered by COMPETE are able to describe simultaneously, without taking into account a crossing-odd component of the scattering amplitude, the TOTEM ρ measurement at $\sqrt{s} = 8$ and 13 TeV together with the ensemble of the total cross-section measurements by TOTEM in the $\sqrt{s} = 2.76$ to 13 TeV energy range [1, 11, 49, 50]. The exclusion of the COMPETE published models is clearly illustrated by Figure 2. The same quantitative and qualitative conclusion is reached with a p-value analysis as detailed in ref. [2].

The presence of an Odderon effect in the pair of excitation functions $(\rho(s), \sigma_{\rm tot}(s))$ is further supported by Figure 3, that compares the measured values of ρ and σ_{tot} to two different class of model calculations, indicating the Odderon exchange effects explicitely and directly. Predictions of a model by Nicolescu and collaborators from refs. [18, 19] together with the the Durham or KMR model of Khoze, Martin and Ryshkin [20] (that also included a crossing-odd contribution from ref. [21]) were compared to the reference TOTEM measurements (red dots). These results, summarized on Figure 3, confirm that at $\sqrt{s} = 13$ TeV, the pair of $(\rho, \sigma_{\rm tot})$ data is best described with the help of Odderon effects [2].

5.2 Total, elastic and inelastic cross-sections

Fig. 6 indicates TOTEM results for the differential cross-section of elastic pp scattering at $\sqrt{s} = 2.76$ TeV. The low-t part of the measured distribution is frequently approximated with an exponential,

$$\frac{d\sigma}{dt} = A \, \exp(Bt), \tag{1}$$

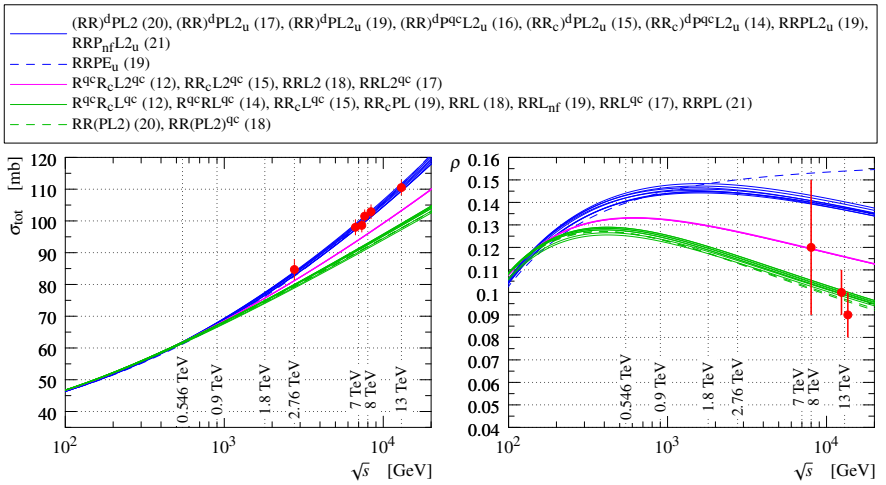

Figure 2. COMPETE bands for the total cross-section $\sigma_{tot}(s)$ and the $\rho(s)$ indicate [16] that without an Odderon contribution, recent TOTEM data at $\sqrt{s}$ = 13 TeV for the pair of (σ_{tot}, ρ) cannot be described simultaneously.

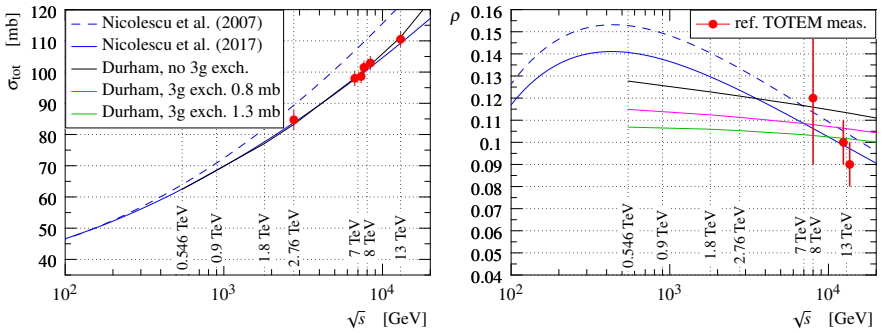

Figure 3. Measured values of σ_{tot} and ρ are compared to two different class of model calculations. The comparisons indicate that with an Odderon contribution, the recent TOTEM data for the pair of $(\sigma_{\rm tot}, \rho)$ at $\sqrt{s}$ = 13 TeV can be described simultaneously: Predictions of the Odderon model by Nicolescu and collaborators are shown by a dashed [18] and solid blue curves [19]. Results from the KMR model [20] without Odderon effects are shown with a black line, and with Odderon effects are shown with magenta and green lines, where the crossing-odd contribution is taken from ref. [21]. Reference TOTEM measurements are indicated by red dots.

with the values of B and R indicated on Fig. 6. The B and R results of TOTEM are summarized for $\sqrt{s}$ = 2.76 TeV and 13 TeV in Table 2. Here ratio R is defined as $R = max/min$, this quantity characterizes the dip-bump region of the differential cross-section of elastic scattering beyond the domain of eq. (1). The ratio R is the ratio of the value of the differential cross section at the (first) diffractive maximum and minimum, denoted here as *max* and *min*, respectively.

Two comments are due. The first of these comments is that eq. (1) corresponds to an exponential “diffractive cone" approximation, that may be valid in the low-t domain only.

This equation corresponds to the so called "Grey Gaussian" approximation, that suggests a relationship between the nuclear slope parameter B, the real to imaginary ratio ρ_0, the total cross-section $\sigma_{\rm tot}$ and the elastic cross-section $\sigma_{\rm el}$ as follows [22, 24, 44]:

$$A = B\sigma_{\rm el} = \frac{1+\rho_0^2}{16\pi}\sigma_{\rm tot}^2, \qquad B = \frac{1+\rho_0^2}{16\pi}\frac{\sigma_{\rm tot}^2}{\sigma_{\rm el}}. \tag{2}$$

Let us note that in the present notation we suppress the s-dependence of the observables, ie. $\sigma_{\rm tot} \equiv \sigma_{\rm tot}(s)$, $\sigma_{\rm el} \equiv \sigma_{\rm el}(s)$ etc. The above relationships, in a slightly modified form, have been utilized by TOTEM to measure the total cross-section by TOTEM using the luminosity independent method at 2.76, 7, 8 and 13 TeV in refs. [1, 9, 11, 51], respectively, based on the following luminosity independent formula:

$$\sigma_{\rm tot} = \sigma_{\rm el} + \sigma_{\rm inel} = \frac{16\pi}{1+\rho_0^2}\frac{\frac{d\sigma}{dt}\big|_{t=0}}{\sigma_{\rm el}+\sigma_{\rm inel}} = \frac{16\pi}{1+\rho_0^2}\frac{\frac{dN}{dt}\big|_{t=0}}{N_{\rm el}+N_{\rm inel}}. \tag{3}$$

Expressing parameters A and B in terms of the elastic and the total cross-section as given in eq. (2) is particularly useful, when we discuss the inelastic profile function called also the shadow profile of the protons, as detailed below.

The second comment relates to the ratio of the elastic to the total cross-section, $\frac{\sigma_{\rm el}}{\sigma_{\rm tot}}$. The shadow profile function is introcuded as $P(b) = 1 - |\exp[-\Omega(b)]|^2$, where $\Omega(b)$ is the so-called opacity function, which is generally complex. It is defined with the help of the relation $t_{\rm el}(b) = i\Big(1 - \exp[-\Omega(b)]\Big)$, where $t_{\rm el}(b)$ stands for the Fourier-Bessel transformed elastic scattering amplitude $T_{\rm el}(\Delta)$, where $\Delta = \sqrt{-t}$ is the modulus of the four-momentum transfer in elastic scattering. For more details on these transformations and convention, see refs. [25–27]. For clarity, let us note that other conventions are also used in the literature and for example the shadow profile $P(b)$ is also referred to as the inelastic profile function as it corresponds to the probability distribution of inelastic proton-proton collisions in the impact parameter b with $0 \le P(b) \le 1$. When the real part of the scattering amplitude is neglected, $P(b)$ is frequently denoted as $G_{\rm inel}(s,b)$, see for example refs. [29, 32, 42, 43, 45].

In the exponential elastic cone approximation of eqs. (1,2), the shadow profile function has a remarkable and very interesting behaviour, as anticipated in ref. [44]:

$$P(b) = 1 - \Big[1 - r\,\exp\Big(-\frac{b^2}{2B}\Big)\Big]^2 - \rho_0^2 r^2\,\exp\Big(-\frac{b^2}{B}\Big), \qquad \text{where} \qquad r = 4\,\frac{\sigma_{\rm el}}{\sigma_{\rm tot}}. \tag{4}$$

Thus the shadow profile at the center, $P_0 = P(b=0)$ reads as

$$P_0 = \frac{1}{1+\rho_0^2} - (1+\rho_0^2)\Big[r - \frac{1}{1+\rho_0^2}\Big]^2, \tag{5}$$

which cannot become maximally absorptive or black ($P_0 = 1$) at those colliding energies, where ρ_0 is not negligibly small. The maximal absorption corresponds to $P_0 = \frac{1}{1+\rho_0^2}$, reached where the ratio of the elastic to total cross-sections reaches the value $r = 1/(1+\rho_0^2)$, corresponding to $4\Big(1+\rho_0^2\Big)\sigma_{\rm el} = \sigma_{\rm tot}$. Given that $\rho_0 \le 0.15$ as indicated on Figure 2 and $\rho(s)$ seems to decrease with increasing energies at least in the $8 \le \sqrt{s} \le 13$ TeV region, the critical value of the elastic to total cross-section ratio corresponds to about $\sigma_{\rm el}/\sigma_{\rm tot} \approx 24.5{-}25.0$ %. Table 1 and the right panel of Figure 4 indicates that this threshold, within errors, is reached approximately already at $\sqrt{s} = 2.76$ TeV. The threshold behavior saturates somewhere between 2.76 and 7 TeV. According to the best COMPETE extrapolation, as indicated on the right panel of

Table 1. Summary of cross-section results of TOTEM at $\sqrt{s}$ = 2.76 and 13 TeV in pp collisions [1, 3, 4, 51].

$\sqrt{s}$ (TeV)	σ_{tot} (mb)	σ_{el} (mb)	σ_{in} (mb)	σ_{el}/σ_{tot} (%)
2.76	84.7 ± 3.3	21.8 ± 1.4	62.8 ± 2.9	25.7 ± 1.1
13.0	110.6 ± 3.4	31.0 ± 1.7	79.5 ± 1.8	28.1 ± 0.9

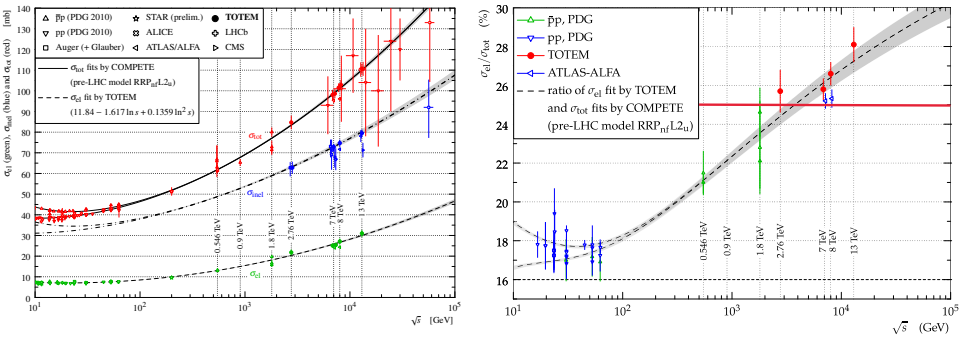

Figure 4. **Left panel:** The total, elastic and inelastic cross-sections as measured at various LHC energies and below. The total cross-section at $\sqrt{s}$ = 13 TeV is determined with ρ = 0.1 at this energy. Overview of total (σ_{tot}), inelastic (σ_{el}) and elastic (σ_{el}) cross-sections for pp and $p\overline{p}$ collisions as a function of $\sqrt{s}$, including TOTEM measurements over the whole energy range explored by the LHC. Uncertainty band on theoretical models and/or fits are described in the Legend. The continuous black lines (lower for pp, upper for $p\overline{p}$) represent the best fits of the total cross section data by the COMPETE collaboration. The dashed line results from a fit of the elastic scattering data. The dash-dotted lines refer to the inelastic cross section and are obtained as the difference between the continuous and dashed fits. From refs. [1, 2]. **Right panel:** The elastic to total cross-section ratio increases with increasing energies, as indicated on this Figure from ref. [1]. At the LHC energies between 8 and 13 TeV it crosses significantly the important limit of $(1+\rho_0^2)\sigma_{el}/\sigma_{tot} = 1/4$. It is important to note that this ratio reaches the critical value in the region of $\sqrt{s}$ = 2.76 – 7 TeV and it clearly exceeds it at $\sqrt{s}$ = 13 TeV. The best COMPETE fit suggests a threshold behaviour in the region of $\sqrt{s}$ = 2.76 - 4 TeV.

Figure 4 , such a transition may happen around the threshold energy of $\sqrt{s_{\rm th}} \approx 2.76 - 4$ TeV. As indicated on this right panel of Figure 4, the elastic to total cross-section ratio becomes significantly larger than the threshold value at $\sqrt{s}$ = 13 TeV colliding energies.

It follows that the inelastic or shadow profile function of the proton undergoes a qualitative change in the region of $2.76 < \sqrt{s} < 7$ TeV energies. The investigation of such a dip or hollowness, corresponding to $\sigma_{\rm el} \geq \sigma_{\rm tot}/4/\left(1+\rho_0^2\right)$ according to Equation 4, is a hotly debated, current topic in the literature. At high energies, with $\sigma_{\rm el} \geq \sigma_{\rm tot}/4$, hollowness may become a generic property of the shadow profile functionsthat characterize the impact parameter distribution of inelastic scatterings. The maximum of $P(s, b = 0) \approx 1$ at $\sigma_{\rm el}(s) \approx \sigma_{\rm tot}(s)/4$ seems to be rather independent of the detailed b-dependent shape of the inelastic collisions, see for example ref. [44]. We recommend refs. [23, 24, 29–33] for early papers as well as refs. [34–45] for more recent theoretical discussions on this apparently rather fundamental-looking nature of proton-proton scattering at LHC and asymptotic energies.

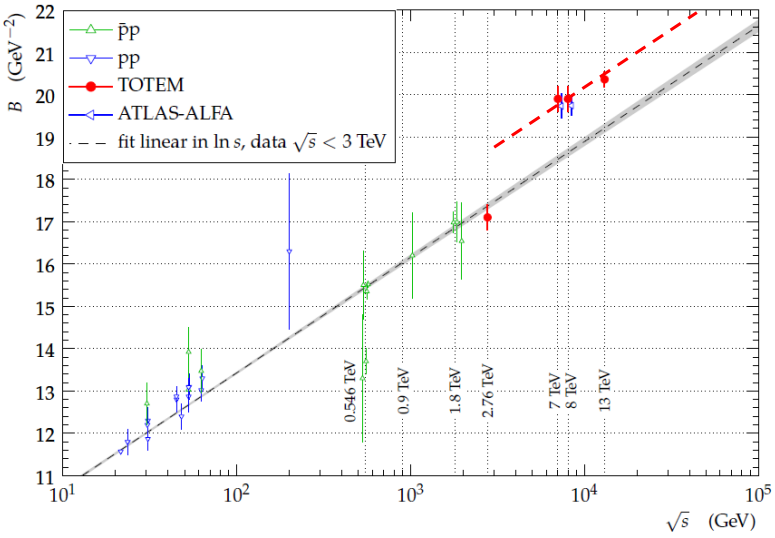

Figure 5. Excitation function of the slope parameter B in elastic proton-proton scattering. The TOTEM data at 2.76, 7, 8 and 13 TeV suggest the opening of a new channel between $\sqrt{s} = 2.76$ and 7 TeV, as noted in ref. [1] and indicated qualitatively by the red dashed line.

Table 2. Summary of B and R measurements of TOTEM at $\sqrt{s} = 2.76$ and 13 TeV in pp collisions [1, 3, 4, 51].

$\sqrt{s}$ (TeV)	B (GeV^{-2})	R
2.76	17.1 ± 0.3	1.7 ±0.2
13.0	20.40 ±0.01$^{\text{syst}}$ ± 0.002$^{\text{stat}}$	1.77 ±0.01$^{\text{stat}}$

5.3 B and R measurements

Recent TOTEM measurements of the nuclear slope parameter B and the diffractive maximum-to-minimum ratio R are summarized and discussed in this sub-section.

The growth of B as well as the growth of σ_{tot} with increasing collision energies $\sqrt{s}$ is characterizing the universal properties of proton-proton scattering and indicate the dominance of a colorless exchange. The most recent TOTEM measurements on the nuclear slope parameter at $\sqrt{s} = 2.76$ and 13 TeV are summarized in Table 2. It is quite remarkable that the excitation function of nuclear slope parameter $B(s)$ at $\sqrt{s} = 2.76$ TeV follows closely the trends of nuclear slopes measured before below the TeV energy scale, as shown on the summary plot for $B(s)$ on Figure 5.

Earlier TOTEM results of the nuclear slope parameter B measured at $\sqrt{s} = 7$ and 8 TeV corresponded to results above the low-energy trend, while the B value measured at 2.76 TeV follows the low-energy trends. The most recent TOTEM result for B at $\sqrt{s} = 13$ TeV confirms the new trend seen already at 7 and 8 TeV. Thus TOTEM result on $B(s)$ suggests the opening of a new physics channel or a new domain of proton-proton scattering, that starts slightly above 2.76 TeV but below 7 TeV. These results are fully consistent with the threshold behaviour of the elastic to total cross-section ratio, that reaches the treshold called refractive scattering domain and the development of a hollow inside the proton at $\sqrt{s_{\text{th}}} \approx 2.76 - 4.0$ TeV, as indicated on the right panel of Figure 4.

5.4 Differential elastic cross section measurements at $\sqrt{s} = 2.76$ and 13 TeV

Detailed measurements of the differential cross-section of elastic pp and $p\overline{p}$ measurements indicate that the nearly exponential cone behaviour is first of all only approximately exponential, precision measurements reveal a non-exponential component. Such a non-exponential feature of the elastic differential cross-section was reported first, as far as we know, in high statistics $\pi^+ p$, $\pi^- p$ and pp collisions at an incident-beam momentum of 200 GeV/c in the FNAL - E - 0069 experiment [46] and was also reviewed in ref. [47]. TOTEM found a significant, more than 7σ effect, in high precision measurements of the elastic pp scattering at $\sqrt{s} = 8$ TeV [49, 50]. The analysis of the hadronic part of the scattering amplitude outside the CNI region resulted in an observation of the non-exponential diffractive cone effect also in pp elastic scattering at the currently highest available energy of $\sqrt{s} = 13$ TeV, see Table 5 and Figure 13 of ref. [2].

This non-exponential feature is followed by a diffractive minumum and a diffractive maximum in elastic pp collisions. It is important to note, that no secondary minimum or maximum structure is observed, although the TOTEM acceptance extends to several times $t_{\rm min}$, the t-value corresponding to the diffractive minimum both at 7 and 13 TeV. According to the investigations of Czyz and Maximon of elastic scattering of composite particles in multiple diffraction theory, a single diffractive minimum corresponds to $(2, 2)$ elastic scattering: if the symmetric scattering objects contain more than two sub-structures, more than a single diffractive minimum develops [48]. These ideas were elaborated for asymmetric internal structures in the framework of the quark-diquark model of protons by Bialas and Bzdak [25, 26]. This model came in two variants, in one case the proton is assumed to be a weakly bound state of a quark or diquark, abbreviated as $p = (q, d)$, but the internal structures of the quarks and diquarks are unresolved. In this case the pp elastic scattering develops indeed a single minimum, in agreement with the observations from the ISR energy of $\sqrt{s} = 23.5$ GeV up to the LHC energy of 7 TeV, after a small real part is added to the elastic scattering amplitude in a unitarized way [26]. If the diquark were resolved as a weekly bound state of two quarks, $d = (q, q)$ and $p = (q, (q, q))$ t at least two diffractive minima would become observable in the $0 \leq -t \leq 2.5$ GeV^2 kinematic domain, while experimentally only a single diffractive minimum is observed. This dip region is followed by a diffractive maximum or bump, continued in a monotonically decreasing and apparently structureless tail.

In the region of the diffractive minimum and maximum, a third order polynomial fit was utilized to extract the value of the differential cross-section at the diffractive maximum and minimum. The left panel of Fig. 6 indicates that the ratio R of diffractive maximum to diffractive minimum can be determined in pp reactions at $\sqrt{s} = 2.76$ TeV reasonably well. This left panel of Fig. 6 shows two different third order polynomial fits, that indicate that the ratio R is rather stable for the choice of the fitting function, however the position of the diffractive maximum is rather uncertain and more data with better statistics, and if possible at larger values of t are desirable to determine precisely the position of the diffractive maximum as a function of t.

The right panel of Fig. 6 also compares the differential cross-section measurement of TOTEM at $\sqrt{s} = 2.76$ TeV for elastic pp scattering with the similar measurement of the D0 collaboration for $p\overline{p}$ elastic scattering at the slightly lower energy of $\sqrt{s} = 1.96$ TeV [8]. This Figure indicates that $R = 1.0 \pm 0.1$ for $p\overline{p}$ elastic scattering at Tevatron energies. The same plot also shows that the t-dependent slope parameter $B(t)$ is clearly different for proton-proton and proton-antiproton elastic scattering in the $-t \approx 0.4$ GeV^2 region, the difference being 2.6 $\pm$ 0.56 GeV^{-2}, a more than 4σ effect.

Fig. 7 indicates TOTEM data for the differential cross-section of elastic pp scattering at $\sqrt{s} = 13$ TeV, from ref. [3]. The systematic error range is indicated with a yellow band. The

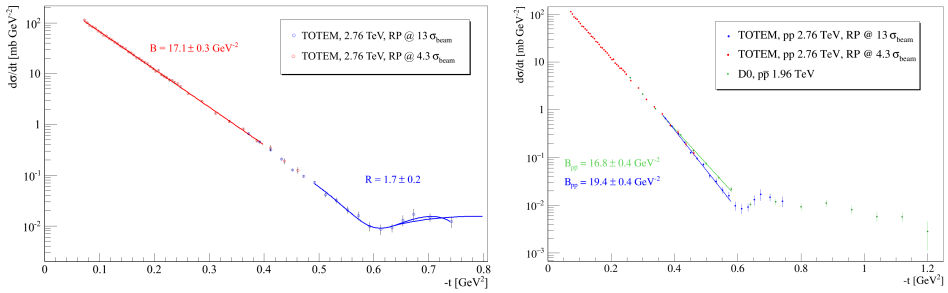

Figure 6. Left panel: Differential cross-section of elastic pp scattering measured at the LHC energy of $\sqrt{s} = 2.76$ TeV by TOTEM, as compared to third order polynomial fits in the dip and bump region [4]. The nuclear slope parameter is $B = 17.1 \pm 0.3$ GeV^{-2}, the maximum/minimum ratio is $R = 1.7 \pm 0.2$ for this pp dataset. **Right panel:** Differential cross-section of elastic pp scattering measured at the LHC energy of $\sqrt{s} = 2.76$ TeV by TOTEM [4], as compared to D0 data on elastic proton-antiproton scattering at the Tevatron energy of $\sqrt{s} = 1.96$ TeV [8]. The nuclear slope parameter "swings" ie increases at about $-t \approx 0.4$ GeV^{-2} up to $B_{pp} = 19.4 \pm 0.4$ GeV^{-2} in pp at $\sqrt{s} = 2.76$ TeV, while it remains within errors constant in the $p\overline{p}$ dataset of D0 at the comparable $\sqrt{s} = 1.96$ TeV in the same $-t$ region, $B_{p\overline{p}} = 16.8 \pm 0.4$ GeV^{-2}. The maximum/minimum ratio is $R = 1.0 \pm 0.0$ for the D0 $p\overline{p}$ dataset. Figure from ref. [4].

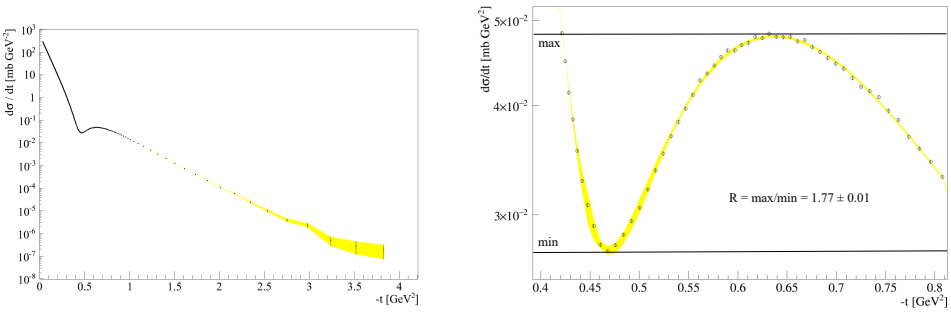

Figure 7. Left panel: TOTEM data for the differential cross-section of elastic pp scattering at $\sqrt{s} = 13$ TeV, from ref. [3]. The statistical and $|t|$-dependent correlated systematic uncertainty envelope is indicated by a yellow band. **Right panel:** The same TOTEM data for the differential cross-section of elastic pp scattering at $\sqrt{s} = 13$ TeV as on the left panel, but zooming in to the dip-and-bump region.

bump/dip ratio is found to be $R = 1.77 \pm 0.01$ which is significantly different from a value of approximately 1.0 ± 0.1, as seen for $p\bar{p}$ elastic scattering at $\sqrt{s} = 1.96$ TeV. The deviation of R in elastic pp collisions from that of elastic $p\overline{p}$ collisions can be interpreted as an Odderon effect, if one can verify that the variation of its excitation function $R(s)$ due to the change of the energy of the collisions can be shown to be negligibly small between 2.76 TeV, the lowest $\sqrt{s}$ value investigated by TOTEM at the LHC and 1.96 TeV, the highest value where elastic $p\overline{p}$ reactions have been measured by D0 at the Tevatron energies [8].

Recently, the sensitivity of the t-dependent elastic slope parameter $B(t)$ to Odderon effects was pointed out in refs. [27, 28, 53], based on a model-independent Lévy expansion method. These observations were confirmed in a model-dependent calculation that uses the maximal

Odderon picture [54]. Similar conclusions were obtained using the Reggeized versions of the Phillips-Barger model, in refs. [55, 56]. Both of these results emphasized the effects of the Odderon contribution, by filling up the region of the diffractive minimum in $p\overline{p}$ reactions, when the calculations are performed in the LHC energy range.

Let us close the discussion of the differential cross-section of elastic pp scattering at the LHC energy range by pointing out that Brodsky and Farrar predicted the asymtotic, large s dependence of the differential cross-section at a fixed value of t in ref. [57]. Such a behaviour can be readily converted to the large-t asymptotic behaviour of the differential cross-section at a fixed value of s as $\frac{d\sigma}{dt} \propto t^{-n}$, where the exponent $n = NDF - 2$ corresponds to the internal degrees of freedom in the incoming and outgoing particles. If the proton is a bound state of 3 dressed quarks, $p = (q, q, q)$ then the number of degrees of freedom is $NDF = 4 \times 3 = 12$ and the exponent n is expected to be of the order of 10. Currently at the largest available t range at $\sqrt{s} = 13$ TeV, the exponent still seems to be fit range dependent, with approximate values of the order of 10.

6 Summary and conclusions

This manuscript reviewed the most recent results of the CERN LHC experiment TOTEM, achieved at the center-of-mass energy scales of $\sqrt{s} = 2.76$ and 13 TeV.

A clear experimental observation of a threshold effect is reported on the collision energy dependence of the nuclear slope parameter $B(s)$, that is found to undergo an abrupt increase in the energy range between $\sqrt{s} = 2.76$ TeV and 7 TeV. A similar but more indirect threshold effect is also reported in the energy dependence of the ratio of the elastic to the total cross-section, $\sigma_{\rm el}(s)/\sigma_{\rm tot}(s)$, which seems to pass the important threshold of 1/4 also in the same energy region. Several theoretical considerations suggest that passing this threshold may result in a fundamental change in the shadow profile of proton-proton collisions, corresponding to the probability distribution of inelastic collisions in the impact parameter space.

Odderon effects were first identified by TOTEM in the $\sqrt{s}$ dependent ($\sigma_{\rm tot}$, ρ) excitation functions. Theoretical models including the effects of the Odderon [17–19], have predicted the observed effects and were able to describe both the pp TOTEM data and the D0 data of $p\overline{p}$ on the TeV scale. As far as we know, there are no models which are able to describe these data without the effects of the Odderon exchange [16, 20, 21].

Subsequently, even more significant Odderon effects were identified by TOTEM in the shape analysis of the differential cross-section. At each of the LHC energies of 13, 7 TeV and 2.76 TeV, the diffractive minimum and maximum has been observed by TOTEM, with a fairly energy independent maximum to minimum ratio of $R = 1.77 \pm 0.01$, 1.7 ± 0.1 and 1.7 ± 0.2, respectively. Thus the diffractive minimum and maximum ratio is apparently a permanent structure with approximately constant magnitude in pp elastic scattering at LHC energies, and such a structure is apparently missing in $p\overline{p}$ collisions at the TeV scale [8]. Therefore, unless something unknown happens between $\sqrt{s}$ =2.76 TeV and 1.96 TeV, the difference between the shape of the pp and $p\overline{p}$ differential cross-sections provides a promising signal of a crossing-odd component in the forward scattering amplitude, corresponding to a predominantly 3-gluon bound state exchange in the t-channel of the proton-proton elastic scattering [4]. The clarification of the significance of these effects is a subject of a D0-TOTEM common publication, which is in preparation at the time of the closing of this manuscript.

Acknowledgments:

T. Cs. would like to express his gratitude to the Organizers of ISMD 2018 for an invitation, partial support and in particular for an outstanding, inspiring and useful meeting and

to thank G. Gustafson and R. Pasechnik for inspiring discussions and kind hospitality at the University of Lund, Sweden. T. Cs. was partially supported by the COST Action CA15213, THOR Project of the European Union, and by the Hungarian NKIFH grants FK-123842 and FK-123959. This research has been partially supported by the Institutions of the TOTEM Collaboration, and the US NSF, the Magnus Ehrnrooth Foundation (Finland), the Waldemar von Frenckell Foundation (Finland), the Academy of Finland, the Finnish Academy of Science and Letters, the Circles of Knowledge Club (Hungary) and the OTKA NK 101438 and the EFOP-3.6.1-16-2016-00001 grants (Hungary).

References

[1] G. Antchev *et al.* [TOTEM Collaboration], Eur. Phys. J. C **79**, no. 2, 103 (2019)
[2] G. Antchev *et al.* [TOTEM Collaboration], arXiv:1812.04732 [hep-ex]
[3] G. Antchev *et al.* [TOTEM Collaboration], arXiv:1812.08283 [hep-ex]
[4] G. Antchev *et al.* [TOTEM Collaboration], arXiv:1812.08610 [hep-ex]
[5] A. M. Sirunyan *et al.* [CMS and TOTEM Collaborations], JHEP **1807**, 153 (2018)
[6] G. Anelli *et al.* [TOTEM Collaboration], JINST **3**, S08007 (2008)
[7] TOTEM Collaboration, *"TOTEM Upgrade Proposal,"* CERN-LHCC-2013-009, LHCC-P-007
[8] V. M. Abazov *et al.* [D0 Collaboration], Phys. Rev. D **86**, 012009 (2012)
[9] G. Antchev *et al.* [TOTEM Collaboration], Phys. Rev. Lett. **111**, no. 1, 012001 (2013)
[10] G. Antchev *et al.*, EPL **96**, no. 2, 21002 (2011)
[11] G. Antchev *et al.* [TOTEM Collaboration], EPL **101**, no. 2, 21004 (2013)
[12] G. Antchev *et al.* [TOTEM Collaboration], EPL **101**, no. 2, 21002 (2013)
[13] G. Antchev *et al.* [TOTEM Collaboration], EPL **101**, no. 2, 21003 (2013)
[14] G. Antchev *et al.* [TOTEM Collaboration], New J. Phys. **16**, 103041 (2014)
[15] C. Patrignani *et al.* [Particle Data Group], Chin. Phys. C **40**, no. 10, 100001 (2016)
[16] J. R. Cudell *et al.* [COMPETE Collaboration], Phys. Rev. Lett. **89**, 201801 (2002)
[17] L. Lukaszuk and B. Nicolescu, Lett. Nuovo Cim. **8**, 405 (1973)
[18] R. Avila, P. Gauron and B. Nicolescu, Eur. Phys. J. C **49**, 581 (2007)
[19] E. Martynov and B. Nicolescu, Phys. Lett. B **778**, 414 (2018)
[20] V. A. Khoze, A. D. Martin and M. G. Ryskin, Phys. Rev. D **97**, no. 3, 034019 (2018)
[21] E. M. Levin and M. G. Ryskin, Phys. Rept. **189**, 267 (1990)
[22] M. M. Block, Phys. Rept. **436**, 71 (2006)
[23] S. M. Troshin and N. E. Tyurin, Int. J. Mod. Phys. A **22**, 4437 (2007)
[24] D. A. Fagundes and M. J. Menon, Nucl. Phys. A **880**, 1 (2012)
[25] A. Bialas and A. Bzdak, Acta Phys. Polon. B **38**, 159 (2007)
[26] F. Nemes, T. Csörgő and M. Csanád, Int. J. Mod. Phys. A **30**, no. 14, 1550076 (2015)
[27] T. Csörgő, R. Pasechnik and A. Ster, Eur. Phys. J. C **79**, no. 1, 62 (2019)
[28] T. Csörgő, R. Pasechnik and A. Ster, arXiv:1811.08913 [hep-ph]
[29] I. M. Dremin and V. A. Nechitailo, Nucl. Phys. A **916**, 241 (2013)
[30] A. Alkin, E. Martynov, O. Kovalenko and S. M. Troshin, Phys. Rev. D **89**, no. 9, 091501 (2014)
[31] S. M. Troshin and N. E. Tyurin, Int. J. Mod. Phys. A **29**, no. 26, 1450151 (2014)
[32] I. M. Dremin, Phys. Usp. **58**, no. 1, 61 (2015)
[33] V. V. Anisovich, V. A. Nikonov and J. Nyiri, Phys. Rev. D **90**, no. 7, 074005 (2014)
[34] E. Ruiz Arriola and W. Broniowski, Phys. Rev. D **95**, no. 7, 074030 (2017)

[35] S. M. Troshin and N. E. Tyurin, Mod. Phys. Lett. A **31**, no. 13, 1650079 (2016)
[36] J. L. Albacete and A. Soto-Ontoso, Phys. Lett. B **770**, 149 (2017)
[37] W. Broniowski and E. Ruiz Arriola, Acta Phys. Polon. B **48**, 927 (2017)
[38] W. Broniowski and E. Ruiz Arriola, Acta Phys. Polon. Supp. **10**, 1203 (2017)
[39] S. M. Troshin and N. E. Tyurin, Int. J. Mod. Phys. A **32**, no. 17, 1750103 (2017)
[40] I. M. Dremin, Usp. Fiz. Nauk **188**, no. 4, 437 (2018) [Phys. Usp. **61**, no. 4, 381 (2018)]
[41] S. D. Campos and V. A. Okorokov, arXiv:1807.02061 [hep-ph]
[42] I. M. Dremin and V. A. Nechitailo, Eur. Phys. J. C **78**, no. 11, 913 (2018)
[43] V. A. Petrov and A. P. Samokhin, Int. J. Mod. Phys. Conf. Ser. **47**, 1860097 (2018)
[44] W. Broniowski, L. Jenkovszky, E. Ruiz Arriola, I. Szanyi, Phys. Rev. D **98**, no. 7, 074012 (2018)
[45] I. Dremin, MDPI Physics **1**, no. 1, 33 (2019)
[46] A. Schiz *et al.*, Phys. Rev. D **24**, 26 (1981)
[47] K. A. Goulianos, Phys. Rept. **101**, 169 (1983)
[48] W. Czyz and L. C. Maximon, Annals Phys. **52**, 59 (1969)
[49] G. Antchev *et al.* [TOTEM Collaboration], Nucl. Phys. B **899**, 527 (2015)
[50] G. Antchev *et al.* [TOTEM Collaboration], Eur. Phys. J. C **76**, no. 12, 661 (2016)
[51] F. J. Nemes, PoS DIS **2017**, 059 (2018)
[52] T. Csörgő [TOTEM Collaboration], EPJ Web Conf. **120**, 02004 (2016)
[53] T. Csörgő, R. Pasechnik and A. Ster, arXiv:1902.00109 [hep-ph]
[54] E. Martynov and B. Nicolescu, arXiv:1808.08580 [hep-ph]
[55] A. Ster, L. Jenkovszky and T. Csörgő, Phys. Rev. D **91**, no. 7, 074018 (2015)
[56] V. P. Gonçalves and P. V. R. G. Silva, arXiv:1811.12250 [hep-ph]
[57] S. J. Brodsky and G. R. Farrar, Phys. Rev. Lett. **31**, 1153 (1973)